International Journal of Innovation and Scientific Research
ISSN 2351-8014 Vol. 73 No. 1 Jun. 2024, pp. 34-49

http://www.ijisr.issr-journals.org/

Study of the influences of the parameters on an asynchronous motor on starting phase

David Yapele[1] and Andre Boussaibo[2]

[1]Department of Electrical Engineering, Energy and Automation, University of Ngaoundere, National School of Agro-Industrial Sciences, Ngaoundere, Cameroon

[2]Department of Electrical Engineering, University of Ngaoundere, University Institute of Technology, Ngaoundere, Cameroon

ABSTRACT: This paper deals with the influence of parameters of an asynchronous motor on its starting phase. Five electrical parameters of the asynchronous motor are concerned by the present study. These are the stator resistance (Rs), the rotor resistance (Rr), the stator inductance (Ls), the rotor inductance (Lr) and the mutual inductance (M). Two mechanical parameters are also studied. These are the moment of inertia (J) and the number of pole pairs (P). The simulation results show that the starting current decreases with increasing values of each of the parameters such as stator resistance, rotor resistance, stator inductance, rotor inductance and the number of pole pairs. On the other hand, the starting current increases with the increase in the mutual inductance and the moment of inertia. The torque decreases with increasing parameters such as stator resistance, stator inductance, rotor inductance and mutual inductance. On the other hand, the torque increases with the increase in rotor resistance, number of pole pairs and moment of inertia. The variation in the values of the different parameters influences the behavior of the rotor speed differently. Increasing the values of parameters such as stator resistance, stator inductance, rotor inductance and moment of inertia influence the rotational speed of the rotor such that the motor takes more time to reach steady state. Increasing the values of rotor resistance, mutual inductance influences the rotor speed such that not only does the motor take longer to reach steady state, but the speed drops in steady state when the motor is loaded. Increasing the values of the number of pole pairs lowers the rotor speed and the motor takes less time to reach steady state. On the basis of the various results obtained from the simulations, we proceeded to optimize the parameters studied in order to reduce the current and obtain a smooth start but with a minimized start-up time. For this purpose the values obtained are as follows: Rr=5.85Ω; Rs=13.805 Ω; Ls=0.300 H; Lr=0.299 H; J=0.031 Kg.m^2; f=0.001136 N.m/rad/s; P=2; M=0.255 H.

KEYWORDS: Asynchronous motor, starting current, torque, speed, optimization.

1 INTRODUCTION

The asynchronous motor mainly has two operating regimes: the transient regime, also called starting phase, and the permanent regime [1]. During the transient phase, the current drawn by the motor is high and of the order of 6 to 7 times the value of the nominal current [2]. During engine starting, the power supply network must be sized to provide higher intensity of current. This approach is inappropriate for certain types of installations such as those powered by photovoltaic generators of more or less low power or those powered directly by storage batteries [3]. Various techniques are used to reduce the current absorbed during starting [4]. Among the most used techniques we can mainly note the use of control circuits driven by control algorithms such as vector control, scalar control, direct torque control, [5]... In the ideal case, the rotor windings should have high resistances at start-up to increase the power factor; we would then have a higher starting torque and a lower current. On the other hand, in operation, the rotor resistance should be as low as possible to have good efficiency. From these requirements in terms of the magnitude of the rotor resistance, there emerges an opposition depending on whether one is in a transient state or in a steady state [6].

According to Bourgeois and Cogniel (1996), the starting phase of an asynchronous motor consists of speeding up the machine shaft, from stopping to operating speed, avoiding electrical and mechanical hazards (current peaks, voltage drops, mechanical shocks...) [7]. According to Burlaka and al., (2020), the current can be further reduced by increasing the number of starting resistors [8]. Gumilar and al. (2020) worked on three types of starting which mainly act on the motor voltage with a view to reducing the current; These are capacitor bank assisted starting, superconducting fault current limiter starting and static reactive energy compensator starting [9]. As part of this research work, it is a question of evaluating the impact of certain electrical and mechanical parameters on the starting phase. An engine available in the laboratory is chosen as a reference, its parameters are taken as initial conditions for the different simulations.

2 MATERIAL AND METHODS

2.1 MODELLING OF THE ASYNCHRONOUS MOTOR IN TRANSIENT MODE

The model of the three-phase asynchronous motor in the real reference frame is illustrated by the diagram in figure 1 below and the arrangements of the three-phase windings of the stator and the rotor [10].

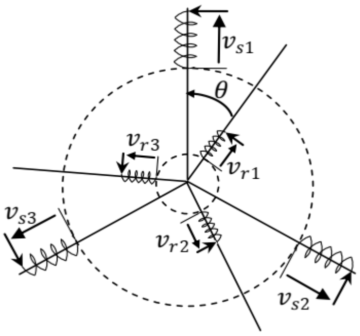

Fig. 1. Arrangement of the three-phase windings of the stator and rotor [11]

To establish relationships between the supply voltages of the asynchronous machine and its primary and secondary currents, we adopt the following hypotheses:

- We neglect the saturation of the magnetic circuit; we neglect the hysteresis losses and the eddy current. This hypothesis makes it possible to easily define the own or mutual inductances of the windings;
- It is assumed that the winding of each phase, both at the stator and at the rotor, creates a flux with sinusoidal distribution. This hypothesis simplifies the expression of the mutual inductances between the phase of the stator and the rotor;
- The construction of the machine is assumed to be symmetrical; the air gap is constant and heating is not taken into account.

These assumptions mean, among other things, that the fluxes are additive, that the natural inductances are constant and that there is a sinusoidal variation of the mutual inductances between the stator windings.

❖ Electrical equations

By applying Ohm’s law to each phase, we can write the o stator and rotor equations as follows:

- Stator equation

$$\begin{cases} v_{s1} = R_s i_{s1} + \frac{d}{dt}(\Phi_{s1}) \\ v_{s2} = R_s i_{s2} + \frac{d}{dt}(\Phi_{s2}) \\ v_{s3} = R_s i_{s3} + \frac{d}{dt}(\Phi_{s3}) \end{cases} \begin{cases} v_{s1} = R_s i_{s1} + \frac{d}{dt}(\Phi_{s1}) \\ v_{s2} = R_s i_{s2} + \frac{d}{dt}(\Phi_{s2}) \\ v_{s3} = R_s i_{s3} + \frac{d}{dt}(\Phi_{s3}) \end{cases}$$

$$\begin{cases} v_{s1} = R_s i_{s1} + \dfrac{d}{dt}(\Phi_{s1}) \\ v_{s2} = R_s i_{s2} + \dfrac{d}{dt}(\Phi_{s2}) \\ v_{s3} = R_s i_{s3} + \dfrac{d}{dt}(\Phi_{s3}) \end{cases} \tag{1}$$

- Rotor equation

$$\begin{cases} v_{r1} = R_r i_{r1} + \dfrac{d}{dt}(\Phi_{r1}) \\ v_{r2} = R_r i_{r2} + \dfrac{d}{dt}(\Phi_{r2}) \\ v_{r3} = R_r i_{r3} + \dfrac{d}{dt}(\Phi_{r3}) \end{cases} \quad (2)$$

$$\begin{cases} v_{r1} = R_r i_{r1} + \frac{d}{dt}(\Phi_{r1}) \; v_{r1} = R_r i_{r1} + \frac{d}{dt}(\Phi_{r1}) \\ v_{r2} = R_r i_{r2} + \frac{d}{dt}(\Phi_{r2}) \; v_{r2} = R_r i_{r2} + \frac{d}{dt}(\Phi_{r2}) \\ v_{r3} = R_r i_{r3} + \frac{d}{dt}(\Phi_{r3}) \; v_{r3} = R_r i_{r3} + \frac{d}{dt}(\Phi_{r3}) \end{cases} \begin{cases} v_{r1} = R_r i_{r1} + \frac{d}{dt}(\Phi_{r1}) \\ v_{r2} = R_r i_{r2} + \frac{d}{dt}(\Phi_{r2}) \\ v_{r3} = R_r i_{r3} + \frac{d}{dt}(\Phi_{r3}) \end{cases}$$

❖ Magnetic equation

The important consequences of the simplifying assumptions lead to linear relationships between flows and currents such as:

- Stator equation

$$\begin{cases} \Phi_{s1} = l_s i_{s1} + m_s i_{s2} + m_s i_{s3} + m_{r1s1} i_{r1} + m_{r2s1} i_{r2} + m_{r3s1} i_{r3} \\ \Phi_{s2} = l_s i_{s2} + m_s i_{s1} + m_s i_{s3} + m_{r1s2} i_{r1} + m_{r2s2} i_{r2} + m_{r3s2} i_{r3} \\ \Phi_{s3} = l_s i_{s3} + m_s i_{s1} + m_s i_{s2} + m_{r1s3} i_{r1} + m_{r2s3} i_{r2} + m_{r3s3} i_{r3} \end{cases}$$

$$\begin{cases} \Phi_{s1} = l_s i_{s1} + m_s i_{s2} + m_s i_{s3} + m_{r1s1} i_{r1} + m_{r2s1} i_{r2} + m_{r3s1} i_{r3} \\ \Phi_{s2} = l_s i_{s2} + m_s i_{s1} + m_s i_{s3} + m_{r1s2} i_{r1} + m_{r2s2} i_{r2} + m_{r3s2} i_{r3} \\ \Phi_{s3} = l_s i_{s3} + m_s i_{s1} + m_s i_{s2} + m_{r1s3} i_{r1} + m_{r2s3} i_{r2} + m_{r3s3} i_{r3} \end{cases} \quad (3)$$

- Rotor equation

$$\begin{cases} \Phi_{r1} = l_r i_{r1} + m_r i_{r2} + m_r i_{r3} + m_{s1r1} i_{s1} + m_{s2r1} i_{s2} + m_{s3r1} i_{s3} \\ \Phi_{r2} = l_r i_{r2} + m_r i_{r1} + m_r i_{r3} + m_{s1r2} i_{s1} + m_{s2r2} i_{s2} + m_{s3r2} i_{s3} \\ \Phi_{r3} = l_r i_{r3} + m_r i_{r1} + m_r i_{r2} + m_{s1r3} i_{s1} + m_{s2r3} i_{s2} + m_{s3r3} i_{s3} \end{cases} \quad (4)$$

Where:

$[\mathcal{L}_s] = \begin{bmatrix} l_s & m_s & m_s \\ m_s & l_s & m_s \\ m_s & m_s & l_s \end{bmatrix}$ and $[\mathcal{L}_r] = \begin{bmatrix} l_r & m_r & m_r \\ m_r & l_r & m_r \\ m_r & m_r & l_r \end{bmatrix}$ are the matrices of the inductances of the stator and the rotor respectively.

l_s and l_r are the natural inductances of a phase.

m_r and m_s are the mutual inductances between two phases of the same armature.

$[M_{rs}] = \begin{bmatrix} m_{r_1s_1} & m_{r_2s_1} & m_{r_3s_1} \\ m_{r_1s_2} & m_{r_2s_2} & m_{r_3s_2} \\ m_{r_1s_3} & m_{r_2s_3} & m_{r_3s_3} \end{bmatrix}$ and $[M_{sr}] = [M_{rs}]^t$ are the matrices of mutual inductances between a phase of one armature and a phase of the other armature such as:

$$\begin{cases} m_{r_is_j} = M_{\max} \cos\left(\theta + (i-j)\frac{2\pi}{3}\right) \\ m_{s_ir_j} = M_{\max} \cos\left(\theta + (j-i)\frac{2\pi}{3}\right) \end{cases} \text{with } i = 1,2,3 \text{ et } j = 1,2,3 \quad (5)$$

θ is the mechanical angle that phase r_i of the rotating armature makes with respect to phase S_i of the fixed armature and p represents the number of pole pairs. By replacing each vector and matrix with these values, we end up with the following overall system:

$$\begin{cases} v_{s1} = R_s i_{s1} + l_s \frac{di_{s1}}{dt} + m_s \frac{di_{s2}}{dt} + m_s \frac{di_{s3}}{dt} + \frac{d}{dt}\left(m_{r_1 s_1} i_{r1} + m_{r_2 s_1} i_{r2} + m_{r_3 s_1} i_{r3}\right) \\ v_{s2} = R_s i_{s2} + l_s \frac{di_{s2}}{dt} + m_s \frac{di_{s1}}{dt} + m_s \frac{di_{s3}}{dt} + \frac{d}{dt}\left(m_{r_1 s_2} i_{r1} + m_{r_2 s_2} i_{r2} + m_{r_3 s_2} i_{r3}\right) \\ v_{s3} = R_s i_{s3} + l_s \frac{di_{s3}}{dt} + m_s \frac{di_{s1}}{dt} + m_s \frac{di_{s2}}{dt} + \frac{d}{dt}\left(m_{r_1 s_3} i_{r1} + m_{r_2 s_3} i_{r2} + m_{r_3 s_3} i_{r3}\right) \\ v_{r1} = R_r i_{r1} + l_r \frac{di_{r1}}{dt} + m_r \frac{di_{r2}}{dt} + m_r \frac{di_{r3}}{dt} + \frac{d}{dt}\left(m_{s_1 r_1} i_{s1} + m_{s_2 r_1} i_{s2} + m_{s_3 r_1} i_{s3}\right) \\ v_{r2} = R_r i_{r2} + l_r \frac{di_{r2}}{dt} + m_r \frac{di_{r1}}{dt} + m_r \frac{di_{r3}}{dt} + \frac{d}{dt}\left(m_{s_1 r_2} i_{s1} + m_{s_2 r_2} i_{s2} + m_{s_3 r_2} i_{s3}\right) \\ v_{r3} = R_r i_{r3} + l_r \frac{di_{r3}}{dt} + m_r \frac{di_{r1}}{dt} + m_r \frac{di_{r2}}{dt} + \frac{d}{dt}\left(m_{s_1 r_3} i_{s1} + m_{s_2 r_3} i_{s2} + m_{s_3 r_3} i_{s3}\right) \end{cases} \tag{6}$$

The system (6) admits a simpler writing since the machine operates in balanced mode where the following relation is verified:

$$i_{s1} + i_{s2} + i_{s3} = 0 \tag{7}$$

And can be rewritten as illustrated by the following system of equation (8):

$$\begin{cases} v_{s1} = R_s i_{s1} + L_s \frac{di_{s1}}{dt} + \frac{d}{dt}\left(m_{r_1 s_1} i_{r1} + m_{r_2 s_1} i_{r2} + m_{r_3 s_1} i_{r3}\right) \\ v_{s2} = R_s i_{s2} + L_s \frac{di_{s2}}{dt} + \frac{d}{dt}\left(m_{r_1 s_2} i_{r1} + m_{r_2 s_2} i_{r2} + m_{r_3 s_2} i_{r3}\right) \\ v_{s3} = R_s i_{s3} + L_s \frac{di_{s3}}{dt} + \frac{d}{dt}\left(m_{r_1 s_3} i_{r1} + m_{r_2 s_3} i_{r2} + m_{r_3 s_3} i_{r3}\right) \\ v_{r1} = R_r i_{r1} + L_r \frac{di_{r1}}{dt} + \frac{d}{dt}\left(m_{s_1 r_1} i_{s1} + m_{s_2 r_1} i_{s2} + m_{s_3 r_1} i_{s3}\right) \\ v_{r2} = R_r i_{r2} + L_r \frac{di_{r2}}{dt} + \frac{d}{dt}\left(m_{s_1 r_2} i_{s1} + m_{s_2 r_2} i_{s2} + m_{s_3 r_2} i_{s3}\right) \\ v_{r3} = R_r i_{r3} + L_r \frac{di_{r3}}{dt} + \frac{d}{dt}\left(m_{s_1 r_3} i_{s1} + m_{s_2 r_3} i_{s2} + m_{s_3 r_3} i_{s3}\right) \end{cases} \tag{8}$$

With $L_s = l_s - m_s$ et $L_r = l_r - m_r$ being the stator and rotor cyclic inductances.

- Mechanical equation

To study the electromechanical phenomenon with a variable rotor speed, it is necessary to add (9), equation of the movement to the previous differential system.

$$\mathrm{J}\frac{\mathrm{d}\Omega}{\mathrm{dt}} = \mathrm{C_e} - \mathrm{C_r} - \mathrm{f_r} \cdot \Omega \tag{9}$$

$$J\frac{d\Omega}{dt} = C_e - C_r - f_r \cdot \Omega$$

Where J: the moment of inertia

Ω: angular speed of rotation of the motor

fr: Coefficient of friction

Ce: Electromagnetic torque

Cr: resistant torque

The electric and magnetic equations which have just been presented are equations which can be used for the study of all regimes, namely: balanced, unbalanced, transient and permanent regime. These equations have a multivariable, non-linear and strongly coupled character leading to the complexity of their resolution. We will use the Park transformation thus making it possible to circumvent this problem and to obtain a system of equations with coefficients independent of the position and therefore to facilitate the resolution, we thus talk of the two-phase model.

2.2 PARK MODELLING OF THE ASYNCHRONOUS MOTOR IN THE FRAME (α, β)

The PARK modeling is built from the electrical equations of the machine [6]. This model uses a certain number of simplifying assumptions. Due to the simplicity of the algebraic formulation, this type of approach is well suited for the modeling of transient phenomena and for the observation of quantities of the asynchronous machine such as currents, torque, and speed [12].

$$\begin{cases} U_{s\alpha} = R_s i_{s\alpha} + \dfrac{d\psi_{s\alpha}}{dt} \\ U_{s\beta} = R_s i_{s\beta} + \dfrac{d\psi_{s\beta}}{dt} \\ 0 = U_{r\alpha} = R_r i_{r\alpha} + \dfrac{d\psi_{r\alpha}}{dt} + \psi_{r\beta}\omega_r \\ 0 = U_{r\beta} = R_r i_{r\beta} + \dfrac{d\psi_{r\beta}}{dt} - \psi_{r\alpha}\omega_r \end{cases} \tag{10}$$

Where:

$$\begin{cases} \psi^{\cdot}_{s\alpha} = L_s i_{s\alpha} + M i_{r\alpha} \\ \psi_{s\beta} = L_s i_{s\beta} + M i_{r\beta} \\ \psi_{r\alpha} = L_r i_{r\alpha} + M i_{s\alpha} \\ \Psi_{r\beta} = L_r i_{r\beta} + M i_{s\beta} \end{cases}$$

By introducing the flow expressions into system (10), we obtain the following system (11):

$$\begin{cases} U_{s\alpha} = R_s i_{s\alpha} + L_s \dfrac{di_{s\alpha}}{dt} + M \dfrac{di_{r\alpha}}{dt} \\ U_{s\beta} = R_s i_{s\beta} + L_s \dfrac{di_{s\beta}}{dt} + M \dfrac{di_{r\beta}}{dt} \\ 0 = R_r i_{r\alpha} + L_r \dfrac{di_{r\alpha}}{dt} + M \dfrac{di_{s\alpha}}{dt} + \omega_r \left(L_r i_{r\beta} + M \cdot i_{s\beta}\right) \\ 0 = R_r i_{r\beta} + L_r \dfrac{di_{r\beta}}{dt} + M \dfrac{di_{s\beta}}{dt} - \omega_r (L_r i_{r\alpha} + M i_{s\alpha}) \end{cases} \tag{11}$$

The system (11) can be expressed in the form of the following differential of (12):

$\frac{d[I]}{dt} = -[L]^{-1}[R][I] + [L]^{-1}[U]$ (12)

With $A = -[L]^{-1}[R]; B = [L]^{-1}$ et $[R] = [R_1] + \omega_r[R_2]$,

$$Where\ [R_1] = \begin{bmatrix} R_s & 0 & 0 & 0 \\ 0 & R_s & 0 & 0 \\ 0 & 0 & R_r & 0 \\ 0 & 0 & 0 & R_r \end{bmatrix} and\ [R_2] = \begin{bmatrix} 0 & 0 & 0 & 0 \\ 0 & 0 & 0 & 0 \\ 0 & M & 0 & L_r \\ -M & 0 & -L_r & 0 \end{bmatrix}$$

We then obtain the following expression (13):

$$\frac{d}{dt}\begin{bmatrix} i_{s\alpha} \\ i_{s\beta} \\ i_{r\alpha} \\ i_{r\beta} \end{bmatrix} = -\begin{bmatrix} L_s & 0 & M & 0 \\ 0 & L_s & 0 & M \\ M & 0 & L_r & 0 \\ 0 & M & 0 & L_r \end{bmatrix}^{-1} \begin{bmatrix} R_s & 0 & 0 & 0 \\ 0 & R_s & 0 & 0 \\ 0 & \omega_r M & R_r & \omega_r L_r \\ -\omega_r M & 0 & -\omega_r L_r & R_r \end{bmatrix} \begin{bmatrix} i_{s\alpha} \\ i_{s\beta} \\ i_{r\alpha} \\ i_{r\beta} \end{bmatrix} + \begin{bmatrix} L_s & 0 & M & 0 \\ 0 & L_s & 0 & M \\ M & 0 & L_r & 0 \\ 0 & M & 0 & L_r \end{bmatrix} \begin{bmatrix} U_{s\alpha} \\ U_{s\beta} \\ 0 \\ 0 \end{bmatrix} \tag{13}$$

The system (13) is the simplified expression of the mathematical model of the asynchronous motor to be modeled in MATLAB/Simulink. The Simulink model of the asynchronous motor based on the system of (13) is that of the figure 2 following:

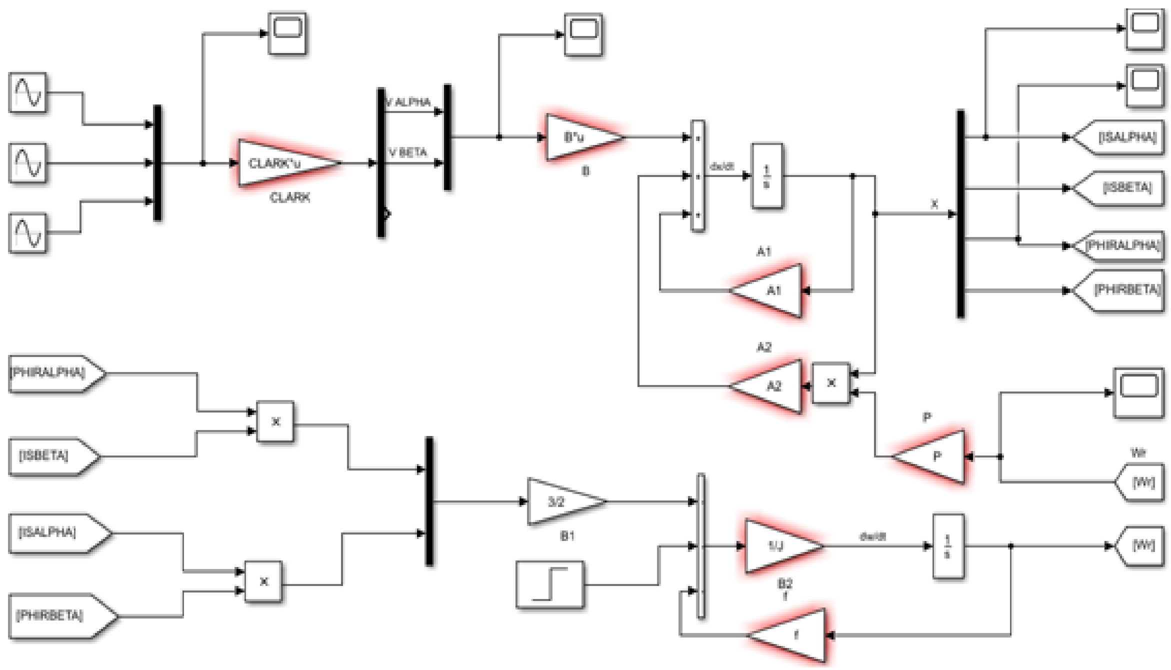

Fig. 2. General simulation diagram

2.3 Setting The Asynchronous Motor

The simulation of the Simulink model in figure 2 takes into account electrical, magnetic and mechanical parameters of the asynchronous machine. In the case of the machine that we take as a model for this work, some of these parameters appear on the nameplate provided by the manufacturer and summarized in table 1 below:

Table 1. Characteristic of the asynchronous motor

Nominal voltage (V)	**220/380**
Rated current (A)	3.7/6.7
Nominal power (kW)	1.5
Number of pole pairs	2
Rated speed (rpm)	1450

The nameplate data alone is not sufficient for simulations of the Simulink model of the induction machine. Tests and measurements were carried out on the asynchronous machine in the laboratory to determine the other electrical and magnetic parameters. Before the actual tests and measurements, it is first a question of schematizing the single-phase equivalent model in figure 3 which summarizes the various parameters characterizing the three-phase asynchronous motor [13].

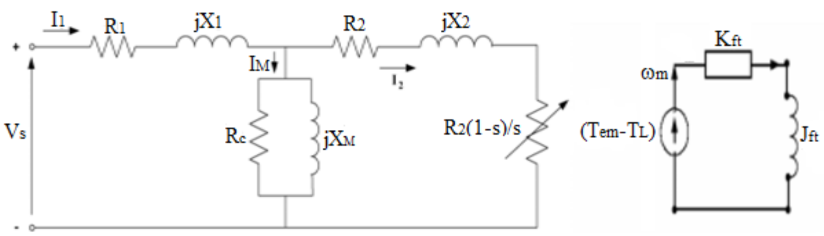

Fig. 3. The single-phase equivalent diagram [13]

The equivalent diagram thus obtained makes it possible to identify all the other parameters remaining and useful for the simulation of the Simulink model in figure 2. The tests and measurements made it possible to obtain the parameters summarized in table 2 below:

Table 2. Parameters of the three-phase asynchronous machine

Stator Resistance Rs (Ω)	3.805
Rotor Resistance Rr (Ω)	4.85
Inductance statorique Ls (H)	0.274
Inductance rotorique Lr (H)	0.274
Mutual Stator/rotor inductance Msr (H)	0.258
Moment of inertia J (Kg/m)	0.031
Coefficient of friction Kf (N.m/rad/s)	0.001136

3 Simulation Results

3.1 Influence Of The Variation Of The Stator Resistance (Rs)

Figures 4, 5 and 6 illustrate the temporal profiles of stator current, torque and speed respectively of the motor. These profiles are obtained for stator resistance values varying from 3.8 to 24 Ω. It can be seen that the increase in stator resistance leads to a reduction in the starting current of the asynchronous motor. This result justifies the hypothesis of McElveen and Toney (2001) regarding starting by elimination of stator resistance [14]. We also note that the increase in stator resistance leads to a reduction in the starting torque of the asynchronous motor; consequently, a smooth start is obtained following the certain reduction of mechanical shocks. The increase in stator resistance influences the rotational speed of the rotor such that the motor takes longer to reach steady state.

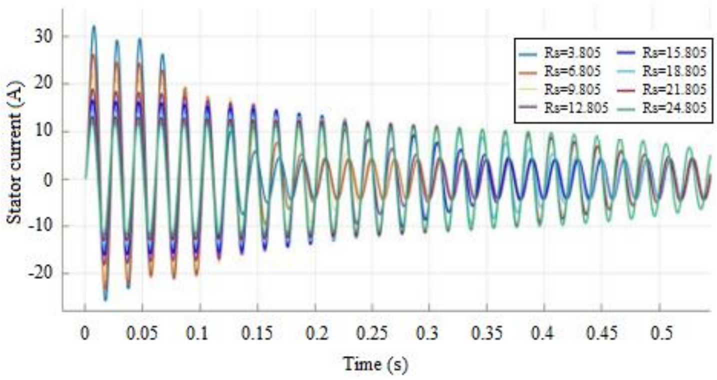

Fig. 4. Temporal profile of stator current

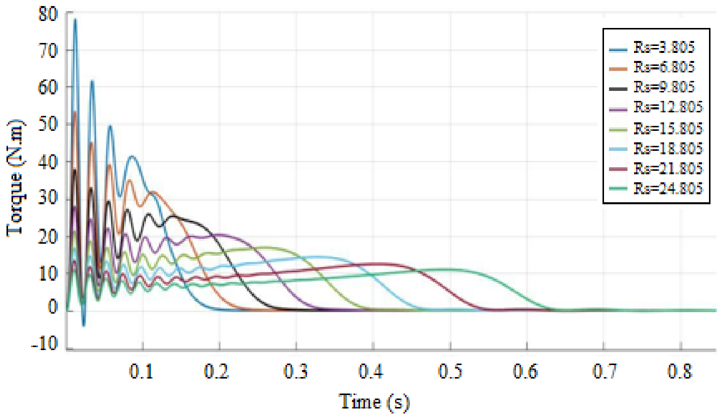

Fig. 5. Temporal profile of the torque

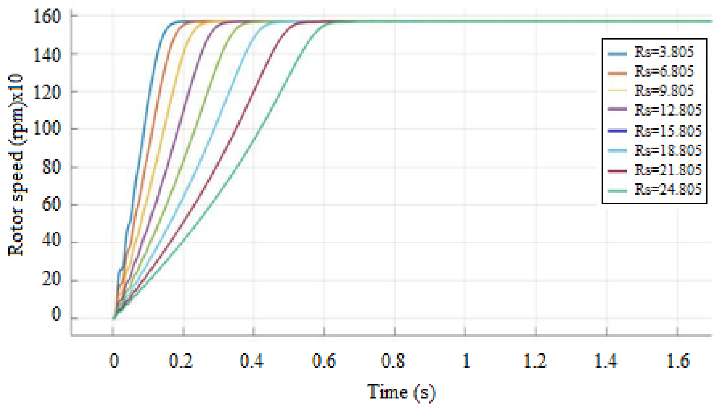

Fig. 6. Temporal profile of speed

3.2 Influence Of The Variation In Rotor Resistance (RR)

Figures 7, 8 and 9 illustrate the temporal profiles of the stator current, torque and speed respectively obtained for the variation of the rotor resistance values from 5.85 to 24.85 Ω. We note that the increase in rotor resistance leads to a reduction in the starting current of the asynchronous motor. On the other hand, we see that the torque increases with the increase in rotor resistance. The increase in rotor resistance influences the rotational speed of the rotor such that the motor takes more time to reach steady state, but less than in the case of stator resistance. Furthermore, we note that the speed drops with the increase in rotor resistance in steady state when the motor is loaded.

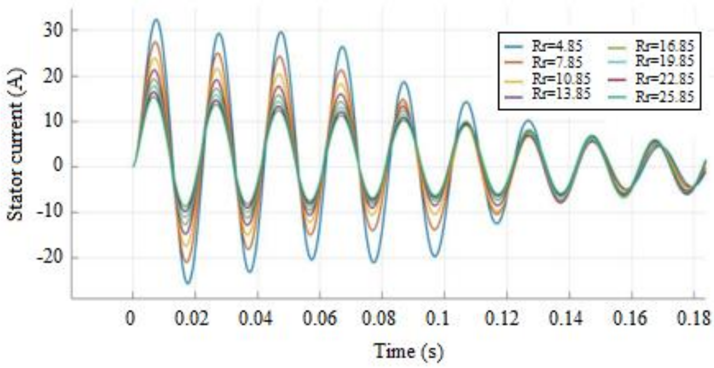

Fig. 7. Temporal profile of stator current

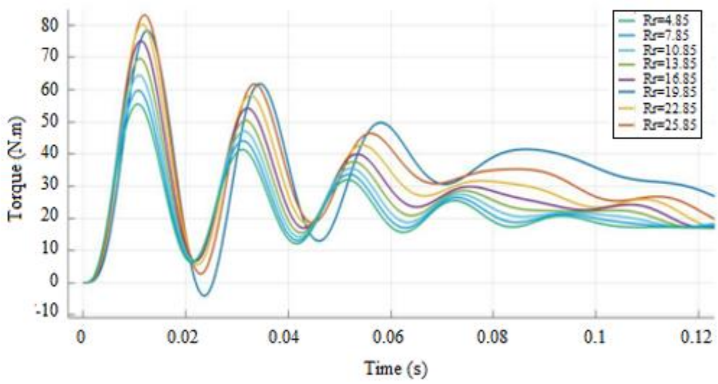

Fig. 8. Temporal profile of torque

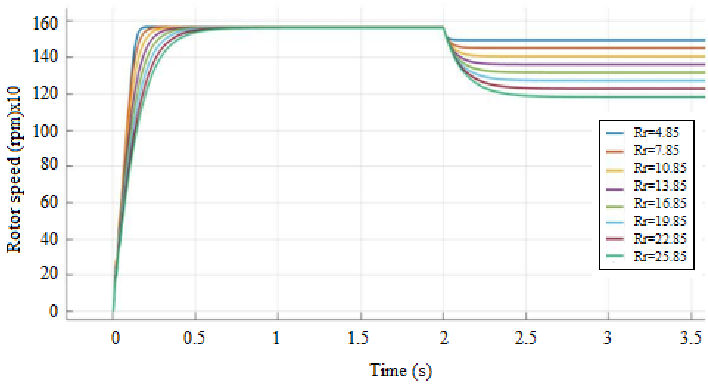

Fig. 9. Temporal profile of speed

3.3 INFLUENCE OF THE VARIATION OF THE STATOR INDUCTANCE (LS)

Figures 10, 11 and 12 illustrate the time profiles of stator current, torque and speed respectively. These profiles are obtained for inductance values varying from 0.27 to 0.43 H. The increase in stator inductance leads to a reduction in current as well as starting torque. We see that the stator inductance is a parameter whose adjustment can reduce mechanical shocks during the start-up phase. The increase in stator inductance influences the rotation speed of the rotor such that the motor takes longer to reach steady state; however, the motor takes less time than in the cases of increases in stator and rotor resistance.

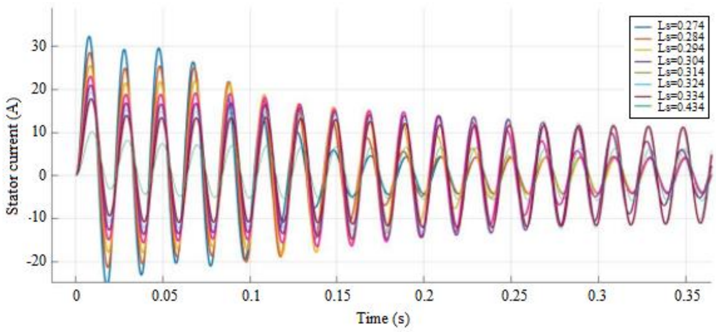

Fig. 10. Temporal profile of stator current

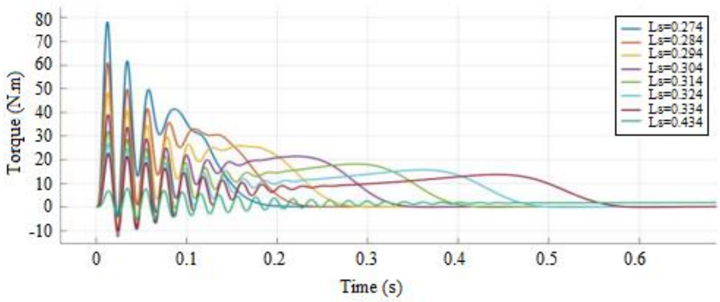

Fig. 11. Temporal profile of torque

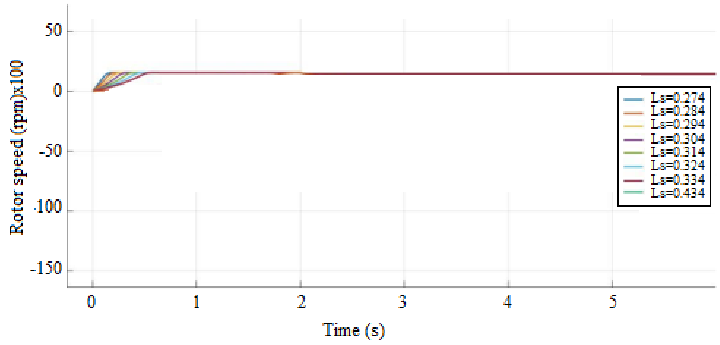

Fig. 12. Temporal profile of speed

3.4 INFLUENCE OF THE VARIATION OF THE ROTOR INDUCTANCE (LR)

Figures 13, 14 and 15 illustrate the temporal profiles of the stator current and the torque at starting and the rotation speed of the motor under variation of the inductance from 0.27 to 0.41 H. We make the same observations as in the case of the stator inductance. The increase in rotor inductance leads to a reduction in current and torque at starting. We can once again see that the rotor inductance is a parameter that can be adjusted to reduce mechanical shocks during the starting phase. The increase in rotor inductance influences the motor speed such that the motor takes a little longer to reach steady state than in the case of stator inductance.

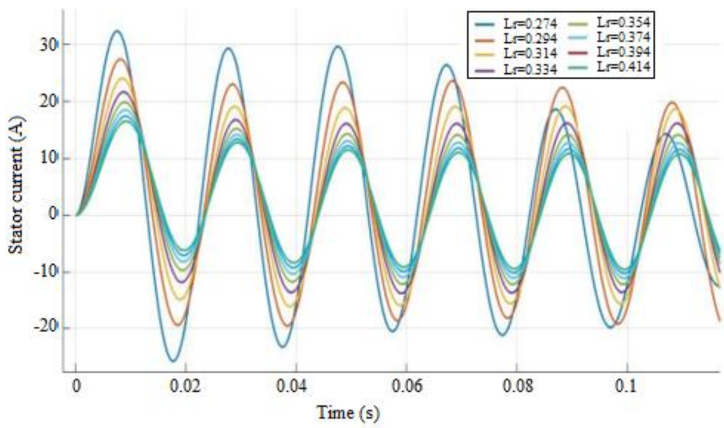

Fig. 13. Temporal profile of stator current

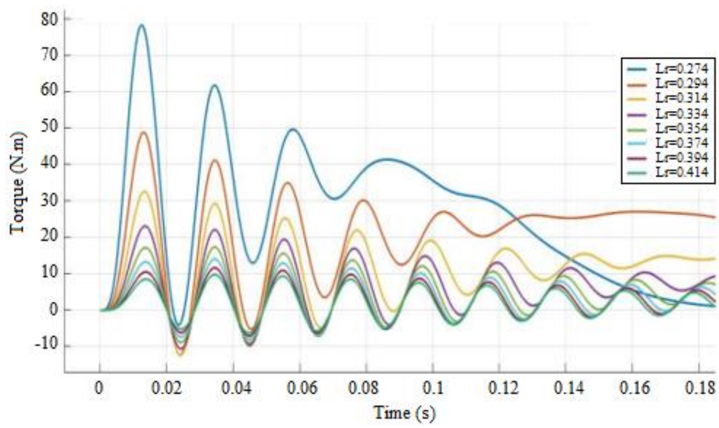

Fig. 14. Temporal profile of torque

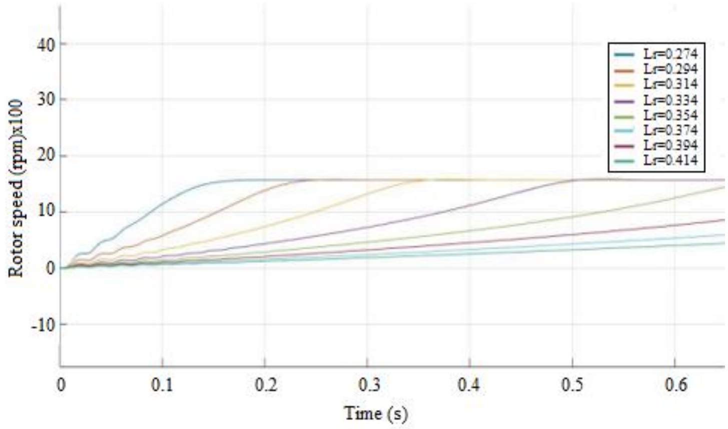

Fig. 15. Temporal profile of speed

3.5 INFLUENCE OF THE VARIATION OF MUTUAL INDUCTANCE (M)

Figures 16, 17 and 18 show the temporal profiles of the starting current and torque and the motor rotation speed. The increase in mutual inductance leads to an increase in starting current and also torque. The increase in mutual inductance influences the speed such that the motor takes longer to reach steady state. Furthermore, the speed decreases with the increase in the mutual in steady state when the motor is loaded.

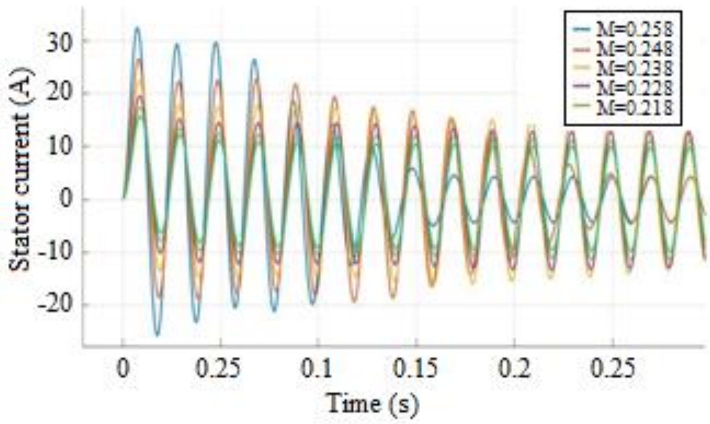

Fig. 16. Temporal profile of stator current

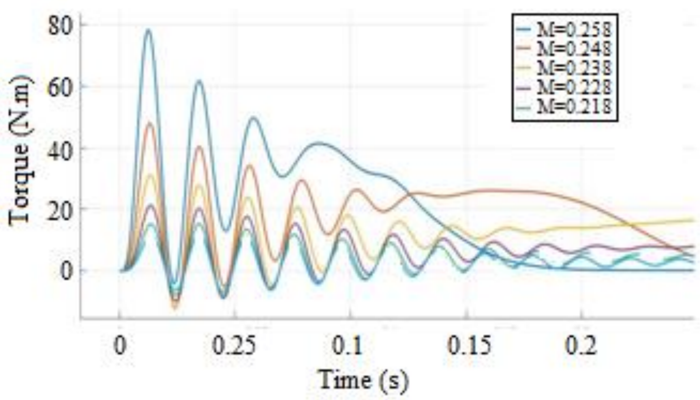

Fig. 17. Temporal profile of torque

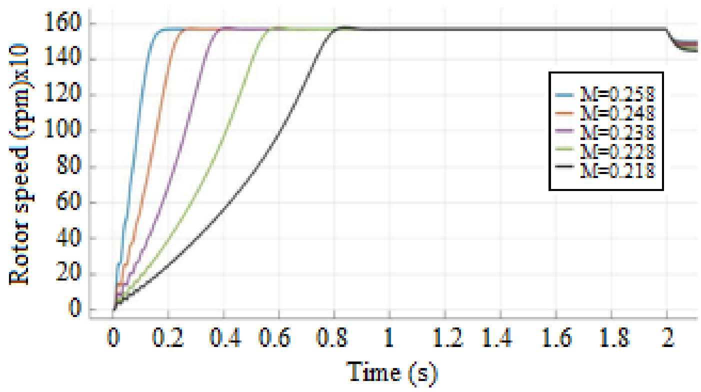

Fig. 18. Temporal profile of speed

3.6 Influence Of Variation In The Number Of Pole Pairs (P)

Figures 19, 20 and 21 illustrate the temporal profiles of the starting current and torque and the motor rotation speed. Increasing the number of pole pairs leads to a decrease in starting current. However, increasing the number of pole pairs increases the starting torque. Consequently, increasing the number of pole pairs increases the mechanical shocks during the start-up phase. We observe that the increase in the number of pole pairs leads to a decrease in the rotation speed of the motor under load. However, the time taken by the motor to reach steady state decreases with this increase.

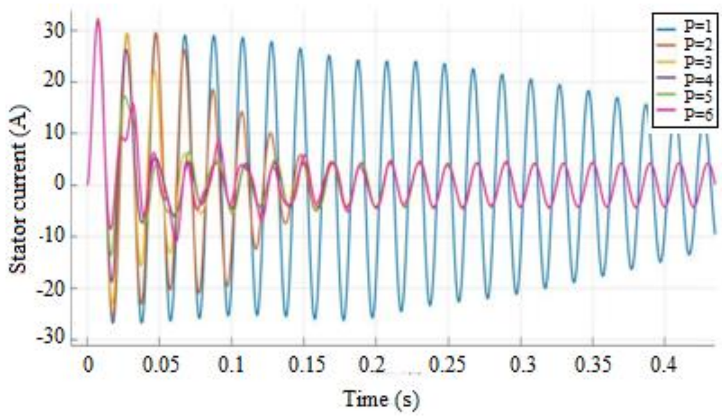

Fig. 19. Temporal profile of stator current

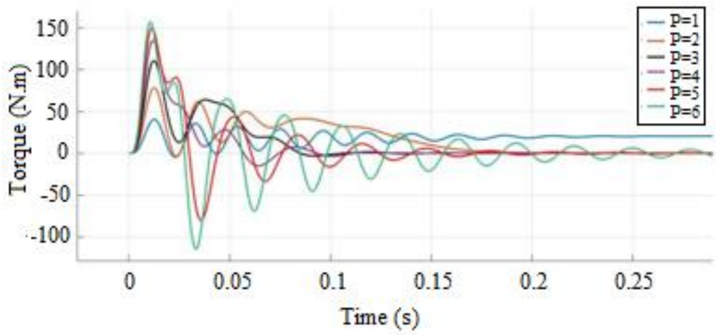

Fig. 20. Temporal profile of torque

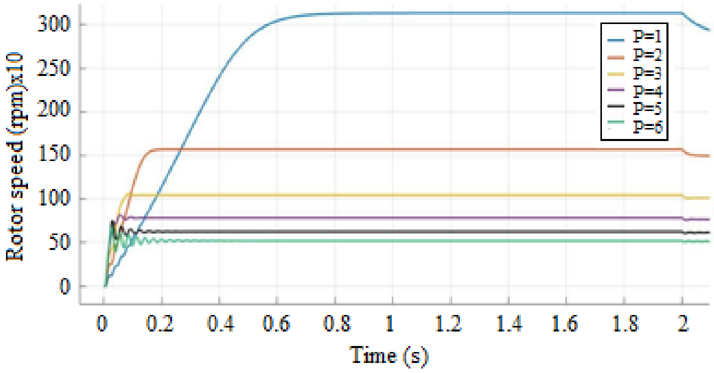

Fig. 21. Temporal profile of speed

3.7 INFLUENCE OF THE VARIATION OF THE MOMENT OF INERTIA (J)

Figures 22, 23 and 24 illustrate the temporal profiles of the starting current and torque and the motor rotation speed. The increase in the moment of inertia leads to an increase in the starting current. This increase in the moment of inertia also increases the starting torque of the asynchronous motor. However, the moment of inertia influences the rotation speed such that the motor takes more time to reach steady state.

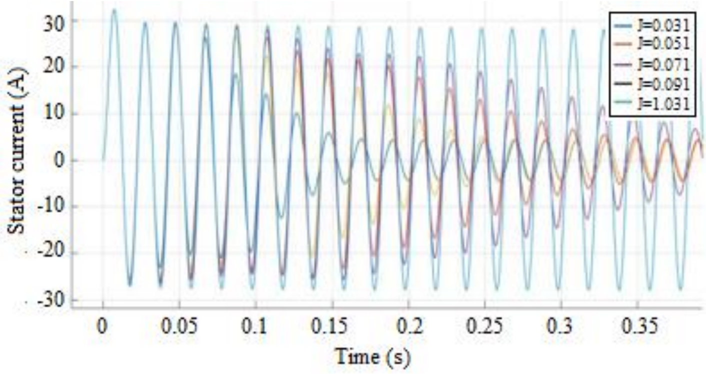

Fig. 22. Temporal profile of stator current

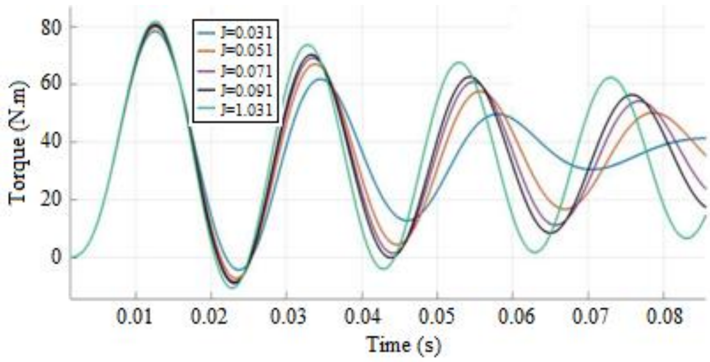

Fig. 23. Temporal profile of torque

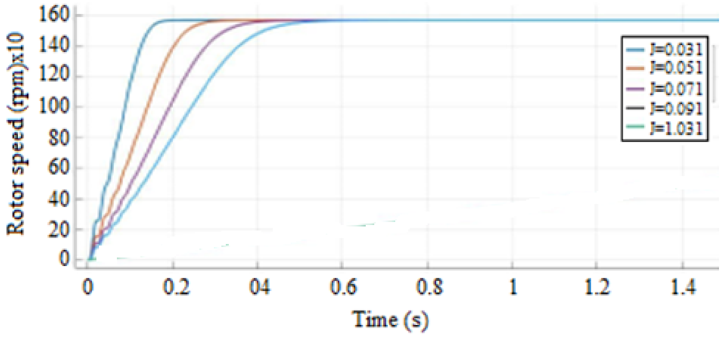

Fig. 24. Temporal profile of speed

4 PARAMETER OPTIMIZATION

4.1 OPTIMIZATION RESULTS BY ADJUSTING LR AND LS

Figures 25, 26 and 27 illustrate the temporal profiles of the current and torque at starting and of the motor rotation speed for adjusted values of the stator and rotor inductances in comparison to the profiles obtained with unadjusted values. The adjusted values are 0.284 H and 0.294 H respectively for the stator inductance and the rotor inductance. By observing the current curves, we see that the current when starting the motor goes from 32 A (without adjustment) to 24 A (with adjustment). The starting torque goes from 80 N.m (without adjustment) to around 40 N.m (with adjustment). Analysis of the speed curves shows that the adjusted values make it possible to obtain a smoother starting compared to starting without adjusting the values.

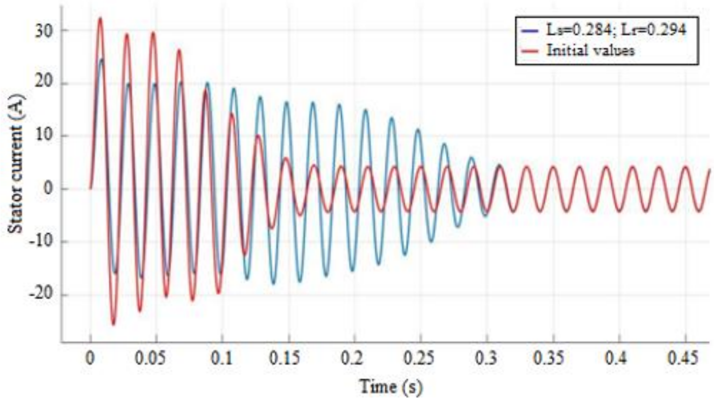

Fig. 25. Temporal profile of stator current

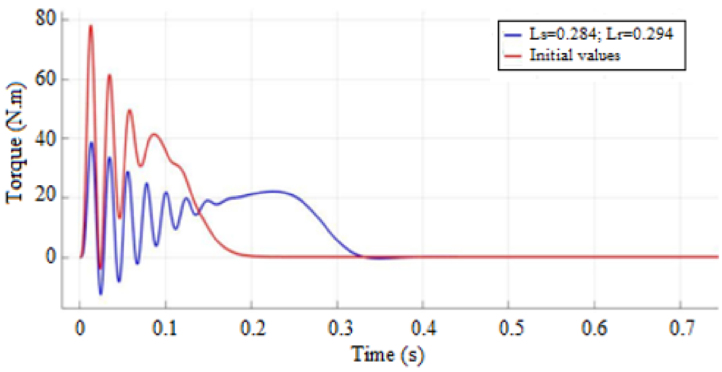

Fig. 26. Temporal profile of torque

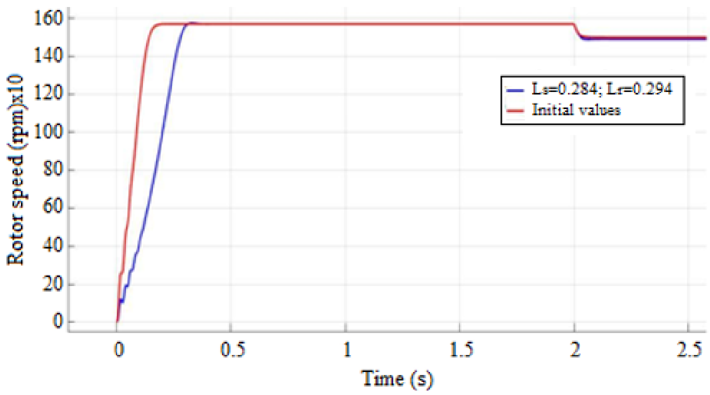

Fig. 27. Temporal profile of speed

4.2 Optimization Results By Adjusting Rr, Rs, Ls And Lr

Figures 31, 32 and 33 illustrate the temporal profiles of the current and torque at starting and of the motor rotation speed for adjusted values of the stator and rotor resistances, of the stator and rotor inductances in comparison to the profiles obtained with non-values. adjusted. By increasing the stator resistance by 1 ohm compared to the different value of the second approach we can lower the starting current of the asynchronous motor from 32 A to only 10 A. which we consider to be optimal. The starting torque is left from a large value represented by the red color to a small value represented in blue estimated at 10 N.m; a torque which can well drive our load which is 10 N.m which is the nominal torque value therefore complete attenuation of mechanical shocks and smoother starting. By adjusting to a larger number of parameters the motor takes longer to reach steady state compared to the natural characteristic. And after applying a load torque, the speed drops to 1350 rpm.

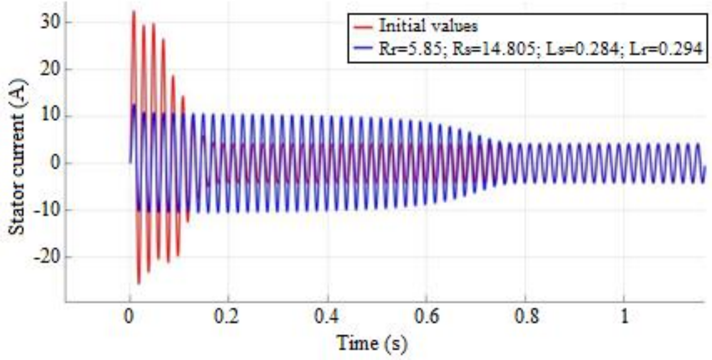

Fig. 28. Temporal profile of stator current

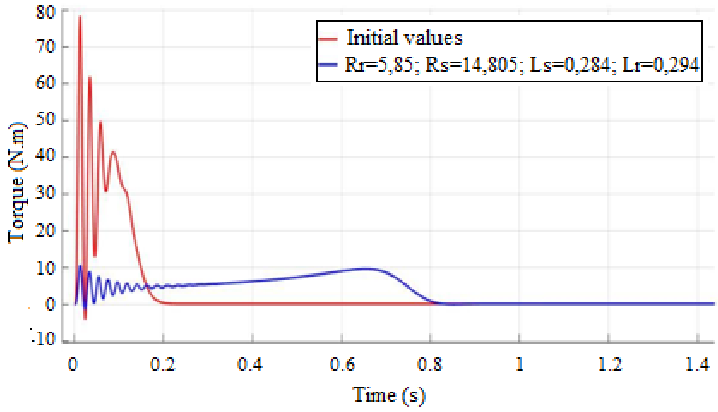

Fig. 29. Temporal profile of torque

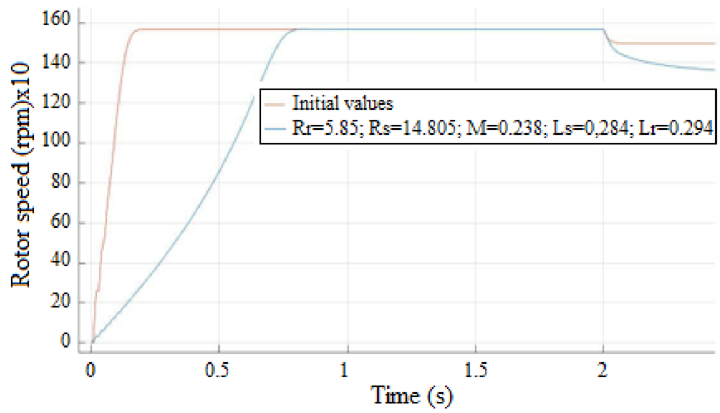

Fig. 30. Temporal profile of speed

5 Conclusion

Simulation tests are carried out on a Simulink model of an asynchronous motor. Studies of the influence of certains electrical, magnetic and mechanical parameters on the motor starting phase have been carried out. The quantities monitored are the stator current, the torque and the rotor speed. It emerges from the analysis of the results obtained that the variation in the values of the different parameters of the motor influences differently the behavior of the quantities monitored at starting. However, there are optimum values of the parameters studied making it possible to obtain from the motor a sufficiently low starting current, a smoother starting and a shorter starting time. The implementation of the results obtained is likely to contribute to the design of motors suitable for photovoltaic applications.

References

[1] S. R. Shaw and S. B. Leeb (1999). « Identification of induction motor parameters from transient stator current measurements ». IEEE Transactions on Industrial Electronics 46 (1): 139-49.J.

[2] J. Lesenne, F. Notelet et G. Seguier (1981). Introduction à l'électrotechnique approfondie. Technique et documentation, 1981.

[3] F. Salama (2011). « Modélisation d'un système multi générateurs photovoltaïques interconnectés au réseau électrique«, Mémoire de Magister, Université Ferhat Abbas – Sétif.

[4] P. S. Nasab, H. Safamehr and M. Moazzami (2013). AV/f=cte control drive for permanent capacitor single-phase induction motor. Iran, Journal of intelligent procedures in electrical technology, Volume 4, N°13, pp. 64-73.

[5] A. Boussaibo, M. Kamta, J. Kayem, D. Toader, S. Haragus and A. Maghet, «Characterization of photovoltaic pumping system model without battery storage by MATLAB/Simulink,» *2015 9th International Symposium on Advanced Topics in Electrical Engineering (ATEE),* Bucharest, Romania, 2015, pp. 774-780, doi: 10.1109/ATEE.2015.7133907.

[6] J. P. Louis (2004). « Modélisation des machines électriques en vue de leur commande: Concepts généraux ». Traité EGEM, série Génie électrique, 2-7462.

[7] R. Bourgeois and D. Cogniel (1996). Mémotech électrotechnique. Educalivre/Casteilla.

[8] B. Vladimir, S. Gulakov and S. Podnebennaya. 2020. « Motor Protection Device For Wound Rotor Induction Machines ». In 2020 IEEE Problems of Automated Electrodrive. Theory and Practice (PAEP), 1-4. IEEE.

[9] L. Gumilar, M. Dezetty, S. Mokhammad and S. N. Rumokoy (2020). « Transient in Electrical Power System under Large Induction Motor Starting Condition ». In 2020 2nd International Conference on Cybernetics and Intelligent System (ICORIS), 1-5. IEEE.

[10] P. Barret (1987). « Régimes transitoires des machines tournantes électriques ».

[11] B. Adkins and R. G. Harley (1975). The general theory of alternating current machine: application to pratical problems. CHAPMAN AND HALL, LONDON.

[12] T. Riad, et H. Benalla (2008). « Contribution à la commande directe du couple de la machine asynchrone. » PhD Thesis, Constantine: Université Mentouri Constantine.

[13] Z. Moussa (2008). « Identification des paramètres et commande vectorielle adaptative à orientation du flux rotorique de la machine asynchrone à cage ». PhD Thesis, Université du Québec à Trois-Rivières.

[14] McElveen, Robbie F, et Michael K Toney. 2001. « Starting high-inertia loads ». IEEE Transactions on Industry Applications 37 (1): 137-44.